The Decay $\Sigma^+ \to p\ell^+\ell^-$ within the Standard Model

Xiao-Gang He[*]

Department of Physics, National Taiwan University, Taipei

Jusak Tandean[†]

Department of Physics and Astronomy,
Wayne State University, Detroit, MI 48201

G. Valencia[‡]

Department of Physics and Astronomy,
Iowa State University, Ames, IA 50011

(Dated: February 2, 2008)

Abstract

The HyperCP collaboration has recently reported the observation of three events for the decay $\Sigma^+ \to p\mu^+\mu^-$. They have suggested that new physics may be required to understand the implied decay rate and the observed $M_{\mu\mu}$ distribution. Motivated by this result, we re-examine this mode within the standard model, considering both the short-distance and long-distance contributions. The long-distance part depends on four complex form-factors. We determine their imaginary parts from unitarity, fix two of the real parts from the $\Sigma^+ \to p\gamma$ measurements, and estimate the other two with vector-meson-dominance models. Taking into account constraints from $\Sigma^+ \to pe^+e^-$, we find that $\Sigma^+ \to p\mu^+\mu^-$ is long-distance dominated and its rate falls within the range suggested by the HyperCP measurement.

[*]Electronic address: `hexg@phys.ntu.edu.tw`
[†]Electronic address: `jtandean@physics.wayne.edu`
[‡]Electronic address: `valencia@iastate.edu`

I. INTRODUCTION

Three events for the decay mode $\Sigma^+ \to p\mu^+\mu^-$ have been recently observed by the HyperCP (E871) collaboration [1] with results that suggest new physics may be needed to explain them. In this paper we re-examine this mode [2] within the standard model.

There are short- and long-distance contributions to this decay. In the standard model (SM), the leading short-distance contribution comes from the Z-penguin and box diagrams, as well as the electromagnetic penguin with the photon connected to the dimuon pair [3]. We find that this contribution yields a branching ratio of order 10^{-12}, which is much smaller than the central experimental value of 8.6×10^{-8} reported by HyperCP [1]. It is well known that the long-distance contribution to the weak radiative mode $\Sigma^+ \to p\gamma$ is much larger than the short-distance contribution. It is therefore also possible to have enhanced long-distance contributions to $\Sigma^+ \to p\mu^+\mu^-$ via an intermediate virtual photon from $\Sigma^+ \to p\gamma$. We find that the resulting branching ratio is in agreement with the measured value. There is, of course, still the possibility [4] that new physics is responsible for the observed branching ratio of $\Sigma^+ \to p\gamma$ and hence that of $\Sigma^+ \to p\mu^+\mu^-$. This implies that it is essential to have an up-to-date estimate of the standard-model contributions, on which we concentrate in this work.

In Sec. II we update the estimate of the short-distance amplitude. We use the standard effective Hamiltonian for the $s \to d\ell^+\ell^-$ transition [3] supplemented with hadronic matrix elements for the relevant currents. In Sec. III we study the long-distance contributions mediated by a real or a virtual photon. These can be parameterized by four (complex) gauge-invariant form-factors [2]. We determine the imaginary parts of these form factors from unitarity. The real parts of two of the form factors can be reasonably assumed to be constant as a first approximation and can then be extracted from the measured rate and asymmetry parameter for $\Sigma^+ \to p\gamma$ up to a fourfold ambiguity. The real parts of the two remaining form-factors cannot be extracted from experiment at present, and so we estimate them using vector-meson-dominance models. Finally, in Sec. IV we combine all these results to present the predictions for the rates and spectra of the two modes $\Sigma^+ \to p\mu^+\mu^-$, pe^+e^-. Before concluding, we discuss the implications of our analysis for the possibility that new physics could be present in the recent measurement by HyperCP.

II. SHORT-DISTANCE CONTRIBUTIONS

The short-distance effective Hamiltonian responsible for $\Sigma^+ \to p\ell^+\ell^-$ contains contributions originating from the Z-penguin, box, and electromagnetic-penguin diagrams. It is given by [3, 5]

$$\mathcal{H}_{\text{eff}} = \frac{G_F}{\sqrt{2}} V_{ud}^* V_{us} \left[(z_{7V} + \tau y_{7V}) O_{7V} + \tau y_{7A} O_{7A} \right] + \frac{G_F}{\sqrt{2}} \sum_j V_{jd}^* V_{js} c_{7\gamma}^j O_{7\gamma} , \tag{1}$$

where V_{kl} are the elements of the Cabibbo-Kobayashi-Maskawa (CKM) matrix [6], z, y, and c are the Wilson coefficients, $\tau = -V_{td}^* V_{ts}/(V_{ud}^* V_{us})$, and

$$
\begin{aligned}
O_{7V} &= \bar{d}\gamma^\mu(1-\gamma_5)s\,\bar{\ell}^-\gamma_\mu\ell^+ , \qquad O_{7A} = \bar{d}\gamma^\mu(1-\gamma_5)s\,\bar{\ell}^-\gamma_\mu\gamma_5\ell^+ , \\
O_{7\gamma} &= \frac{e}{16\pi^2}\,\bar{d}\sigma^{\mu\nu}F_{\mu\nu}\big[m_s(1+\gamma_5) + m_d(1-\gamma_5)\big]s ,
\end{aligned}
\tag{2}
$$

with $F_{\mu\nu}$ being the photon field-strength tensor. The contribution of $O_{7\gamma}$ to $\Sigma^+ \to p\ell^+\ell^-$ occurs via the photon converting to a lepton pair. The total short-distance contribution to the $\Sigma^+ \to p\ell^+\ell^-$ amplitude is then given by

$$
\begin{aligned}
\mathcal{M}(\Sigma^+ \to p\ell^+\ell^-) &= \langle p\ell^+\ell^- |\mathcal{H}_{\text{eff}}|\Sigma^+\rangle \\
&= \frac{G_F}{\sqrt{2}}\Bigg\{ V_{ud}^* V_{us}\big[(z_{7V} + \tau y_{7V})\langle p|\bar{d}\gamma^\mu(1-\gamma_5)s|\Sigma^+\rangle\bar{\ell}^-\gamma_\mu\ell^+ + \tau y_{7A}\langle p|\bar{d}\gamma^\mu(1-\gamma_5)s|\Sigma^+\rangle\bar{\ell}^-\gamma_\mu\gamma_5\ell^+\big] \\
&\quad - \sum_j V_{jd}^* V_{js}\frac{i\alpha\,c_{7\gamma}^j}{2\pi q^2}\big[(m_s + m_d)\langle p|\bar{d}\sigma^{\mu\nu}q_\nu s|\Sigma^+\rangle + (m_s - m_d)\langle p|\bar{d}\sigma^{\mu\nu}q_\nu\gamma_5 s|\Sigma^+\rangle\big]\,\bar{\ell}^-\gamma_\mu\ell^+ \Bigg\} ,
\end{aligned}
\tag{3}
$$

where $q = p_\Sigma - p_p$.

To obtain the corresponding branching ratio, one needs to know the hadronic matrix elements. Employing the leading-order strong Lagrangian in chiral perturbation theory (χPT), given in Eq. (B1), we find

$$
\langle p|\bar{d}\gamma^\mu s|\Sigma^+\rangle = -\bar{p}\gamma^\mu\Sigma , \qquad \langle p|\bar{d}\gamma^\mu\gamma_5 s|\Sigma^+\rangle = (D-F)\,\bar{p}\gamma^\mu\gamma_5\Sigma ,
\tag{4}
$$

where $D = 0.80$ and $F = 0.46$ from fitting to hyperon semileptonic decays, and using quark-model results [7] we obtain

$$
\langle p|\bar{d}\sigma^{\mu\nu}s|\Sigma^+\rangle = c_\sigma\,\bar{p}\sigma^{\mu\nu}\Sigma , \qquad \langle p|\bar{d}\sigma^{\mu\nu}\gamma_5 s|\Sigma^+\rangle = c_\sigma\,\bar{p}\sigma^{\mu\nu}\gamma_5\Sigma ,
\tag{5}
$$

where $c_\sigma = -1/3$. Furthermore, we adopt the CKM-matrix elements given in Ref. [8], the typical Wilson coefficients obtained in the literature [3, 5], namely $z_{7V} = -0.046\alpha$, $y_{7V} = 0.735\alpha$, $y_{7A} = -0.700\alpha$ [3], and $c_{7\gamma}^j$ being dominated by $c_{7\gamma}^c = 0.13$ [5], and the quark masses $m_d = 9\,\text{MeV}$ and $m_s = 120\,\text{MeV}$.

The resulting branching ratio for $\Sigma^+ \to p\mu^+\mu^-$ is about 10^{-12}, which is way below the observed value. There are uncertainties in the hadronic matrix elements, the Wilson coefficients, and the CKM-matrix elements, but these uncertainties will not change this result by orders of magnitude. We therefore conclude that in the SM the short-distance contribution is too small to explain the HyperCP data on $\Sigma^+ \to p\mu^+\mu^-$.

Now, a large branching ratio for $\Sigma^+ \to p\ell^+\ell^-$ may be related to the large observed branching ratio for $\Sigma^+ \to p\gamma$, compared with their respective short-distance contributions. With only the

3

short-distance contribution to $\Sigma^+ \to p\gamma$ within the SM, the branching ratio is predicted to be much smaller than the experimental value [4]. However, beyond the SM it is possible to have an enhanced short-distance contribution to $\Sigma^+ \to p\gamma$ [4] which would enhance the amplitude for $\Sigma^+ \to p\mu^+\mu^-$. The origin of the enhancement may be from new interactions such as W_L-W_R mixing in left-right symmetric models and left-right squark mixing in supersymmetric models [4]. These types of interactions have small effects on other related flavor-changing processes such as K^0-$\bar{K}^0$ mixing, but can have large effects on $\Sigma^+ \to p\gamma$ and therefore also on $\Sigma^+ \to p\ell^+\ell^-$. Thus the observed branching ratio for $\Sigma^+ \to p\gamma$ can be reproduced even if one assumes that there is only the short-distance contribution. More likely, however, the enhancement is due to long-distance contributions within the SM. In the next section we present the most complete estimate possible at present for these long-distance contributions.

III.   LONG-DISTANCE CONTRIBUTIONS

In this section we deal with the contributions to $\Sigma^+ \to p\ell^+\ell^-$ that are mediated by a photon. For a real intermediate photon there are two form factors that can be extracted from the weak radiative hyperon decay $B_i \to B_f \gamma$ and are usually parameterized by the effective Lagrangian

$$\mathcal{L} = \frac{eG_F}{2} \bar{B}_f (a + b\gamma_5) \sigma^{\mu\nu} B_i F_{\mu\nu} . \tag{6}$$

The two form factors, a and b, are related to the width and decay distribution of the radiative decay by

$$\Gamma(B_i \to B_f \gamma) = \frac{G_F^2 e^2}{\pi} \left(|a|^2 + |b|^2 \right) \omega^3 , \tag{7}$$

$$\frac{d\Gamma}{d\cos\theta} \sim 1 + \alpha \cos\theta , \qquad \alpha = \frac{2\,Re\,(ab^*)}{|a|^2 + |b|^2} , \tag{8}$$

where ω is the photon energy, and θ is the angle between the spin of B_i and the three-momentum of B_f. The measured values for $\Sigma^+ \to p\gamma$ are [8]

$$\Gamma(\Sigma^+ \to p\gamma) = (10.1 \pm 0.4) \times 10^{-15} \text{ MeV} , \qquad \alpha = -0.76 \pm 0.08 . \tag{9}$$

When the photon is a virtual one, there are two additional form-factors, and the total amplitude can be parameterized as

$$\mathcal{M}(B_i \to B_f \gamma^*) = -eG_F \bar{B}_f \left[i\sigma^{\mu\nu} q_\mu (a + b\gamma_5) + (q^2 \gamma^\nu - q^\nu \slashed{q})(c + d\gamma_5) \right] B_i \varepsilon_\nu^* , \tag{10}$$

4

where q is the photon four-momentum. We note that the a and c (b and d) terms are parity conserving (violating). The corresponding amplitude for $B_i \to B_f \ell^+ \ell^-$ is then

$$\mathcal{M}(B_i \to B_f \ell^+ \ell^-) = \frac{-ie^2 G_F}{q^2} \bar{B}_f \left(a + b\gamma_5\right) \sigma_{\mu\nu} q^\mu B_i \, \bar{\ell}^- \gamma^\nu \ell^+$$

$$- e^2 G_F \, \bar{B}_f \gamma_\mu (c + d\gamma_5) B_i \, \bar{\ell}^- \gamma^\mu \ell^+ \, , \tag{11}$$

where now $q = p_{\ell^+} + p_{\ell^-}$. In general a, b, c, and d depend on q^2, and for $\Sigma^+ \to p\gamma^*$ the first two are constrained at $q^2 = 0$ by the data in Eq. (9) as

$$|a(0)|^2 + |b(0)|^2 = (15.0 \pm 0.3)^2 \text{ MeV}^2 \, ,$$
$$\text{Re}\left(a(0)\, b^*(0)\right) = (-85.3 \pm 9.6) \text{ MeV}^2 \, . \tag{12}$$

These form factors are related to the ones in Ref. [2] by

$$a = 2ib_1 \, , \qquad b = 2ib_2 \, , \qquad c = \frac{ia_1}{q^2} \, , \qquad d = -\frac{ia_2}{q^2} \, . \tag{13}$$

As we will estimate later on, these form factors have fairly mild q^2-dependence. If they are taken to be constant, by integrating numerically over phase space we can determine the branching ratios of $\Sigma^+ \to p\ell^+\ell^-$ to be, with a and b in MeV,

$$\mathcal{B}(\Sigma^+ \to p\mu^+\mu^-) = \left[2.00\left(|a|^2 + |b|^2\right) - 1.60\left(|a|^2 - |b|^2\right)\right] \times 10^{-10}$$
$$+ \left(1.05\,|c|^2 + 18.2\,|d|^2\right) \times 10^{-6}$$
$$+ \left[0.29\,\text{Re}\,(ac^*) - 16.1\,\text{Re}\,(bd^*)\right] \times 10^{-8} \, , \tag{14a}$$

$$\mathcal{B}(\Sigma^+ \to pe^+e^-) = \left[4.22\left(|a|^2 + |b|^2\right) - 0.21\left(|a|^2 - |b|^2\right)\right] \times 10^{-8}$$
$$+ \left(5.38\,|c|^2 + 15.9\,|d|^2\right) \times 10^{-5}$$
$$+ \left[1.51\,\text{Re}\,(ac^*) - 21.1\,\text{Re}\,(bd^*)\right] \times 10^{-7} \, . \tag{14b}$$

If the form factors have q^2-dependence, the expression is different, and the rate should be calculated with the formula which we give in Appendix A.

A. Imaginary parts of the form factors from unitarity

The form factors which contribute to the weak radiative hyperon decays have been studied in chiral perturbation theory [9–11]. The imaginary parts of a and b for $\Sigma^+ \to p\gamma$ have been determined from unitarity with different results in the literature. Neufeld [9] employed relativistic baryon χPT to find, for $q^2 = 0$,

$$\text{Im}\,a(0) = 2.60 \text{ MeV} \, , \qquad \text{Im}\,b(0) = -1.46 \text{ MeV} \tag{15}$$

in the notation of Eq. (6), whereas Jenkins *et al.* [10] using the heavy-baryon formulation obtained

$$\mathrm{Im}\, a(0) \;=\; 6.18 \text{ MeV} , \qquad \mathrm{Im}\, b(0) \;=\; -0.53 \text{ MeV} . \tag{16}$$

Because of this disagreement, and since we also need the imaginary parts of the form factors c and d, we repeat here the unitarity calculation employing both the relativistic and heavy baryon approaches.

Our strategy to derive the imaginary parts of the four form-factors in Eq. (11) from unitarity is illustrated in Fig. 1. As the figure shows, these imaginary parts can be determined from the amplitudes for the weak nonleptonic decays $\Sigma^+ \to p\pi^0$ and $\Sigma^+ \to n\pi^+$ (the vertex indicated by a square in Fig. 1) as well as the reactions $N\pi \to N\gamma^*$ (the vertex indicated by a blob in Fig. 1). The weak decays have been measured [8], and we express their amplitudes as[1]

$$\mathcal{M}(\Sigma^+ \to N\pi) \;=\; iG_F m_{\pi^+}^2 \, \bar{N}\left(A_{N\pi} - B_{N\pi}\gamma_5\right)\Sigma , \tag{17}$$

where

$$
\begin{aligned}
A_{n\pi^+} &= 0.06 , & B_{n\pi^+} &= 18.53 , \\
A_{p\pi^0} &= -1.43 , & B_{p\pi^0} &= 11.74 .
\end{aligned}
\tag{18}
$$

Following Refs. [9, 10], we adopt the $N\pi \to p\gamma^*$ amplitudes derived in lowest-order χPT.
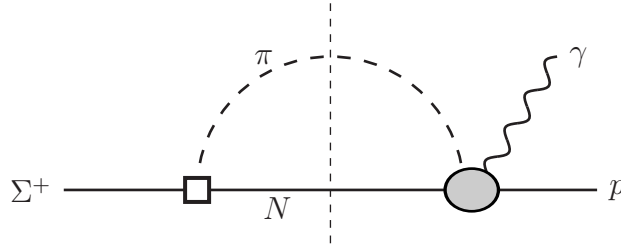

FIG. 1: Unitarity cut.

We present the details of our unitarity calculation in Appendix B. The results in the relativistic and heavy baryon approaches are given in Eqs. (B2) and (B8), respectively. In Fig. 2 we display the two sets of form factors for $0 \le q^2 \le (m_\Sigma - m_N)^2$. We note that, although only the $\Sigma^+ \to n\pi^+$ transition contributes to the heavy-baryon form-factors at leading order, the sizable difference between the $\mathrm{Im}\, a$, or $\mathrm{Im}\, c$, curves arises mainly from relativistic corrections, which reduce the heavy-baryon numbers by about 50%. On the other hand, the difference between the $\mathrm{Im}\, b$, or $\mathrm{Im}\, d$, curves is due not only to relativistic corrections, but also to $A_{n\pi^+}$ being much smaller than $A_{p\pi^0}$.

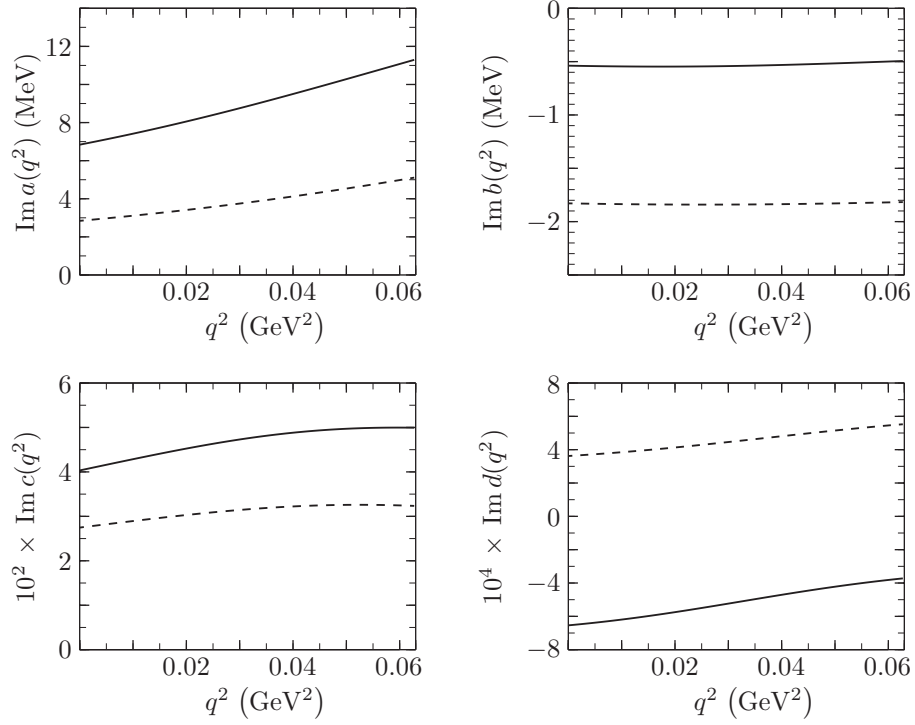[1] We have taken the nonzero elements of γ_5 to be positive.

FIG. 2: Imaginary parts of the form factors in $\Sigma^+ \to p\gamma^*$, obtained using heavy baryon χPT (solid lines) and relativistic baryon χPT (dashed lines).

To compare with the numbers in Eqs. (15) and (16) calculated in earlier work, we find from the relativistic formulas in Eq. (B2)

$$\text{Im}\,a(0) \;=\; 2.84 \text{ MeV} , \qquad \text{Im}\,b(0) \;=\; -1.83 \text{ MeV} , \tag{19}$$

and from the heavy-baryon results in Eq. (B8)

$$\text{Im}\,a(0) \;=\; 6.84 \text{ MeV} , \qquad \text{Im}\,b(0) \;=\; -0.54 \text{ MeV} . \tag{20}$$

Thus our relativistic results are close to those in Eq. (15), from Ref. [9], and our heavy-baryon numbers to those in Eq. (16), from Ref. [10].[2] These two sets of numbers are different for the reasons mentioned in the preceding paragraph.

---

[2] Our heavy-baryon expressions for $\text{Im}\,a(0)$ and $\text{Im}\,b(0)$ are identical to those in Ref. [10], except that their $\text{Im}\,a(0)$ formula has one of the overall factors of $1/(m_\Sigma - m_N)$ apparently coming from their approximating $\left[(m_\Sigma - m_N)^2 - m_\pi^2\right]^{1/2}$ as $m_\Sigma - m_N$. This is the main reason for the value of $\text{Im}\,a(0)$ in Eq. (16) being smaller than that in Eq. (20).

B. Real parts of the form factors

The real parts of the form factors cannot be completely predicted at present from experimental input alone. For $\operatorname{Re} a(q^2)$ and $\operatorname{Re} b(q^2)$, the values at $q^2 = 0$ can be extracted from Eq. (12) after using Eq. (19) or (20) for the imaginary parts. Thus the relativistic numbers in Eq. (19) lead to the four sets of solutions

$$\operatorname{Re} a(0) = \pm 13.3 \text{ MeV}, \quad \operatorname{Re} b(0) = \mp 6.0 \text{ MeV},$$
$$\operatorname{Re} a(0) = \pm 6.0 \text{ MeV}, \quad \operatorname{Re} b(0) = \mp 13.3 \text{ MeV}, \tag{21}$$

while the heavy-baryon results in Eq. (20) imply

$$\operatorname{Re} a(0) = \pm 11.1 \text{ MeV}, \quad \operatorname{Re} b(0) = \mp 7.3 \text{ MeV},$$
$$\operatorname{Re} a(0) = \pm 7.3 \text{ MeV}, \quad \operatorname{Re} b(0) = \mp 11.1 \text{ MeV}. \tag{22}$$

Since these numbers still cannot be predicted reliably within the framework of χPT [9, 10], we will assume that

$$\operatorname{Re} a(q^2) = \operatorname{Re} a(0), \quad \operatorname{Re} b(q^2) = \operatorname{Re} b(0), \tag{23}$$

where the $q^2 = 0$ values are those in Eqs. (21) and (22) in the respective approaches. This assumption is also reasonable in view of the fairly mild q^2-dependence of the imaginary parts seen in Fig. 2, and of the real parts of c and d below. In predicting the $\Sigma^+ \to p\ell^+\ell^-$ rates in the following section, we will use the 8 sets of possible solutions in Eqs. (21) and (22).

The real parts of c and d cannot be extracted from experiment at present. Our interest here, however, is in predicting the SM contribution, and therefore we need to estimate them. To do so, we employ a vector-meson-dominance assumption, presenting the details in Appendix C. The results for $\operatorname{Re} c(q^2)$ and $\operatorname{Re} d(q^2)$ are given in Eqs. (C3) and (C5), respectively. In Fig. 3 we display the two form factors for $0 \leq q^2 \leq (m_\Sigma - m_N)^2$. We can see from Figs. 2 and 3 that c is dominated by its imaginary part, but that d is mostly real.

IV. RESULTS AND CONCLUSIONS

We can now evaluate the rates and spectra of $\Sigma^+ \to p\ell^+\ell^-$ resulting from the various standard-model contributions. Since the short-distance contributions discussed in Sec. II are very small, we shall neglect them. Consequently, the rates are determined by the various form factors in $\Sigma^+ \to p\gamma^*$ calculated in the preceding section and applied in Eq. (A1).

In Table I, we have collected the branching ratios of $\Sigma^+ \to p\mu^+\mu^-$ and $\Sigma^+ \to pe^+e^-$ corresponding to the 8 sets of solutions in Eqs. (21) and (22), under the assumption of Eq. (23) for $\operatorname{Re} a$
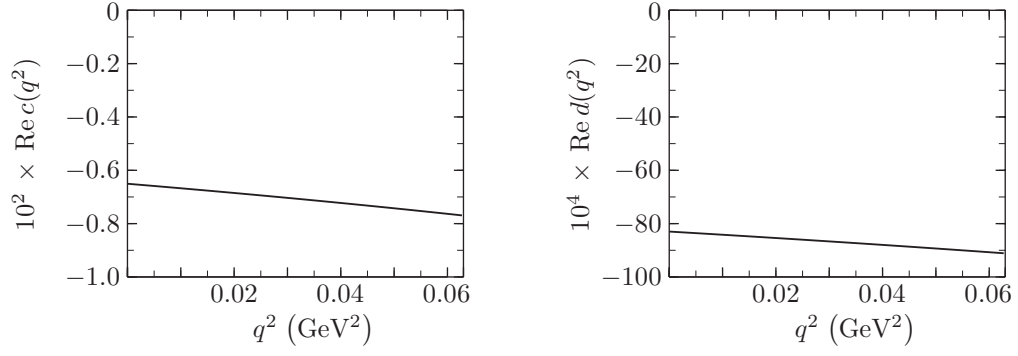
8

FIG. 3: Real parts of c and d.

and $\mathrm{Re}\, b$. The real parts of c and d in Eqs. (C3) and (C5) are used in all the unbracketed branching ratios. For the imaginary parts of the form factors, the expressions in Eq. (B2) [Eq. (B8)] contribute to the unbracketed branching ratios in the upper (lower) half of this table. Within each pair of square brackets, the first number is the branching ratio obtained without contributions from both c and d, whereas the second number is the branching ratio calculated with only the real parts of all the form factors.

TABLE I: Branching ratios of $\Sigma^+ \to p\mu^+\mu^-, pe^+e^-$ in the standard model. The unbracketed branching ratios receive contributions from all the form factors, with the expressions in Eq. (B2) [Eq. (B8)] for the imaginary parts contributing to the numbers in the first (last) four rows. Within each pair of square brackets, the first number has been obtained with $c = d = 0$, and the second with only the real parts of all the form factors.

$\mathrm{Re}\, a$ (MeV)	$\mathrm{Re}\, b$ (MeV)	$10^8\, \mathcal{B}\big(\Sigma^+ \to p\mu^+\mu^-\big)$	$10^6\, \mathcal{B}\big(\Sigma^+ \to pe^+e^-\big)$
13.3	−6.0	1.6 [2.2, 1.3]	9.1 [9.2, 8.6]
−13.3	6.0	3.4 [2.2, 3.1]	9.4 [9.2, 8.8]
6.0	−13.3	5.1 [6.7, 4.7]	9.6 [9.8, 9.0]
−6.0	13.3	9.0 [6.7, 8.6]	10.1 [9.8, 9.5]
11.1	−7.3	2.3 [2.9, 1.5]	9.3 [9.3, 7.2]
−11.1	7.3	4.5 [2.9, 3.7]	9.6 [9.3, 7.5]
7.3	−11.1	4.0 [5.1, 3.2]	9.5 [9.6, 7.4]
−7.3	11.1	7.3 [5.1, 6.4]	10.0 [9.6, 7.8]

In Fig. 4 we show the invariant-mass distributions of the $\mu^+\mu^-$ pair, with $M_{\mu\mu} = \sqrt{q^2}$, that correspond to the smallest and largest rates of $\Sigma^+ \to p\mu^+\mu^-$ listed in Table I for both the relativistic baryon [(a) and (b)] and heavy baryon [(c) and (d)] cases. For $\Sigma^+ \to pe^+e^-$, the mass distributions of the e^+e^- pair, two of which are displayed in Fig. 5, differ very little from each other and are strongly peaked at low $M_{ee} = \sqrt{q^2}$. Also shown in the figures are the distributions obtained with
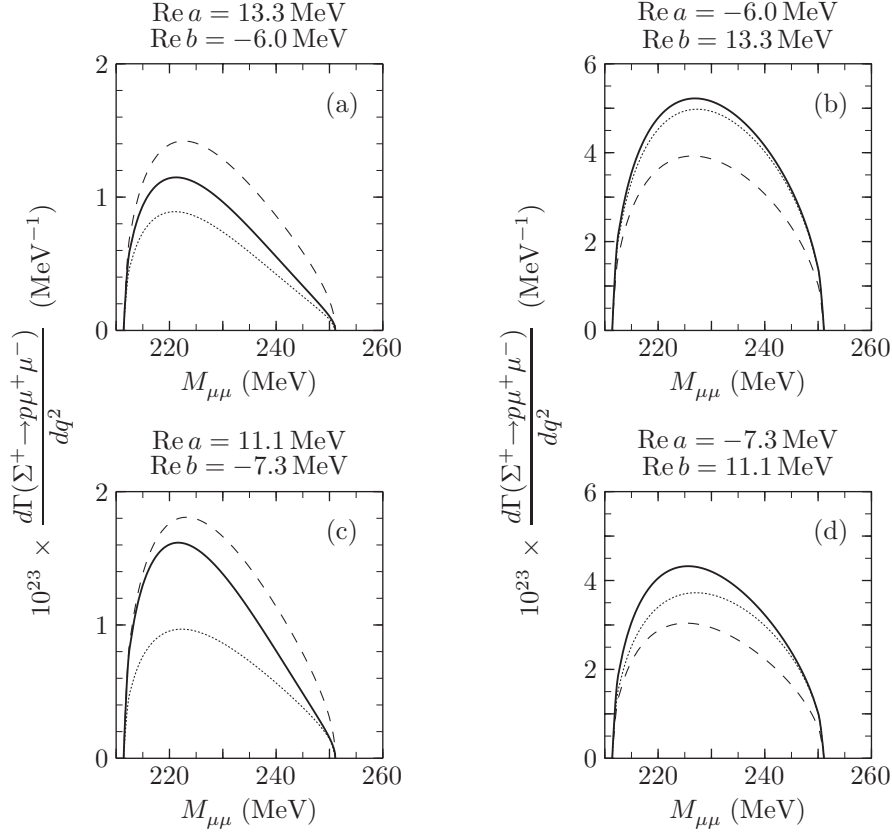
FIG. 4: Invariant-mass distributions of the lepton pair in $\Sigma^+ \to p\mu^+\mu^-$ corresponding to the smallest and largest branching ratios for the (a,b) relativistic and (c,d) heavy baryon cases in Table I. In all distribution figures, each solid curve receives contributions from all the form factors, each dashed curve has been obtained with $c = d = 0$, and each dotted curve involves no imaginary parts of all the form factors.

$c = d = 0$ (dashed curves), as well as those without contributions from the imaginary parts of all the form factors (dotted curves).

We can see from Table I, Fig. 4, and Fig. 5 that the effect of the c and d contributions on the total rates can be up to nearly 40% in $\Sigma^+ \to p\mu^+\mu^-$, but it is much smaller in $\Sigma^+ \to pe^+e^-$. Furthermore, the contributions of the imaginary parts of the form factors can be as large as 35% to the $p\mu^+\mu^-$ rate and roughly 20% to the pe^+e^- rate. This implies that a careful analysis of experimental results, especially in the case of $\Sigma^+ \to p\mu^+\mu^-$, should take into account the imaginary parts of the form factors.

For $\Sigma^+ \to p\mu^+\mu^-$, HyperCP measured the branching ratio to be $\left(8.6^{+6.6}_{-5.4} \pm 5.5\right) \times 10^{-8}$ [1]. It is evident that all the predictions in Table I for the $p\mu^+\mu^-$ mode corresponding to the different sets of form factors fall within the experimental range. For $\Sigma^+ \to pe^+e^-$, the branching ratio can be inferred from the experimental results given in Ref. [12], which reported the width ratio $\Gamma(\Sigma^+ \to$
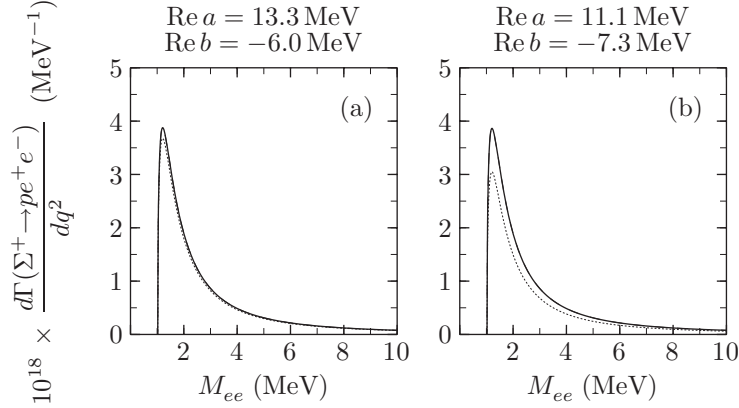
10

FIG. 5: Low-mass portion of the invariant-mass distributions of the lepton pair in $\Sigma^+ \to pe^+e^-$ corresponding to two of the branching ratios in Table I, for the (a) relativistic and (b) heavy baryon cases.

$pe^+e^-)/\Gamma(\Sigma^+ \to p\pi^0) = (1.5 \pm 0.9) \times 10^{-5}$ and interpreted the observed events as proceeding from $\Sigma^+ \to p\gamma^*$, based on the very low invariant-masses of the e^+e^- pair.[3] This number, in conjunction with the current data on $\Sigma^+ \to p\pi^0$ [8], translates into $\mathcal{B}(\Sigma^+ \to pe^+e^-) = (7.7 \pm 4.6) \times 10^{-6}$. Clearly, the results for the pe^+e^- mode in Table I are well within the experimentally allowed range. Based on the numbers in Table I, we may then conclude that within the standard model

$$1.6 \times 10^{-8} \leq \mathcal{B}(\Sigma^+ \to p\mu^+\mu^-) \leq 9.0 \times 10^{-8} ,$$
$$9.1 \times 10^{-6} \leq \mathcal{B}(\Sigma^+ \to pe^+e^-) \leq 10.1 \times 10^{-6} .$$

(24)

The agreement above between the predicted and observed rates of $\Sigma^+ \to p\ell^+\ell^-$ indicates that these decays are dominated by long-distance contributions. However, the predicted range for $\mathcal{B}(\Sigma^+ \to p\mu^+\mu^-)$ is sufficiently wide that we cannot rule out the possibility of a new-physics contribution of the type suggested by HyperCP [1]. Motivated by the narrow distribution of dimuon masses of the events they observed, they proposed that the decay could proceed via a new intermediate particle of mass $\sim 214\,\text{MeV}$, with a branching ratio of $\left(3.1^{+2.4}_{-1.9} \pm 1.5\right) \times 10^{-8}$ [1]. For this hypothesis to be realized, however, the new physics would have to dominate the decay. It will be interesting to see if this hypothesis will be confirmed by future measurements.

Finally, we observe that the smaller numbers $\mathcal{B}(\Sigma^+ \to p\mu^+\mu^-) \sim 2 \times 10^{-8}$ in Table I correspond to the mass distributions peaking at lower masses, $M_{\mu\mu} \sim 220\,\text{MeV}$, in Fig. 4. It is perhaps not coincidental that these numbers are similar to the branching ratio and new-particle mass, respectively, in the HyperCP hypothesis above. This may be another indication that it is not necessary to invoke new physics to explain the HyperCP results.

---

[3] We note that the upper limit of 7×10^{-6} quoted in Ref. [8] and obtained in Ref. [12] is for the presence of weak neutral currents in $\Sigma^+ \to pe^+e^-$ and not for the branching ratio of this mode.

APPENDIX A: DIFFERENTIAL RATE OF $\Sigma^+ \to p\ell^+\ell^-$

If the form factors have q^2-dependence, before integrating over phase space to obtain the branching ratio we should use

$$
\frac{d\Gamma(\Sigma^+ \to p\ell^+\ell^-)}{dq^2 \, dt} = \frac{\alpha^2 G_F^2}{4\pi \, m_\Sigma^3}
$$

$$
\times \left\{ \left[(2m_l^2 + q^2)((m_p - m_\Sigma)^2 - q^2)(m_\Sigma + m_p)^2 + 2q^2 f(m_p, m_\Sigma, m_l, q^2, t) \right] \frac{|a|^2}{q^4} \right.
$$

$$
+ \left[(2m_l^2 + q^2)((m_p + m_\Sigma)^2 - q^2)(m_\Sigma - m_p)^2 + 2q^2 f(m_p, m_\Sigma, m_l, q^2, t) \right] \frac{|b|^2}{q^4}
$$

$$
+ \left[(2m_l^2 + q^2)((m_p - m_\Sigma)^2 - q^2) - 2f(m_p, m_\Sigma, m_l, q^2, t) \right] |c|^2
$$

$$
+ \left[(2m_l^2 + q^2)((m_p + m_\Sigma)^2 - q^2) - 2f(m_p, m_\Sigma, m_l, q^2, t) \right] |d|^2
$$

$$
+ 2(m_\Sigma + m_p)(2m_l^2 + q^2) \left[(m_p - m_\Sigma)^2 - q^2 \right] \frac{\mathrm{Re}\,(ac^*)}{q^2}
$$

$$
\left. - 2(m_\Sigma - m_p)(2m_l^2 + q^2) \left[(m_p + m_\Sigma)^2 - q^2 \right] \frac{\mathrm{Re}\,(bd^*)}{q^2} \right\} , \tag{A1}
$$

where $t = (p_\Sigma - p_{\ell^-})^2$ and

$$
f(m_p, m_\Sigma, m_l, q^2, t) = m_l^4 + (m_p^2 + m_\Sigma^2 - q^2 - 2t)m_l^2 + m_p^2 m_\Sigma^2 - (m_p^2 + m_\Sigma^2)t + (q^2 + t)t ,
$$

with the integration intervals given by

$$
t_{\mathrm{max,min}} = \tfrac{1}{2} \left[m_\Sigma^2 + m_p^2 + 2m_l^2 - q^2 \pm \sqrt{1 - \frac{4m_l^2}{q^2}} \sqrt{(m_\Sigma^2 - m_p^2 - q^2)^2 - 4m_p^2 q^2} \right] , \tag{A2}
$$

$$
q_{\mathrm{min}}^2 = 4m_l^2 , \qquad q_{\mathrm{max}}^2 = (m_\Sigma - m_p)^2 .
$$

It is worth mentioning that, since the form factors belong to the $\Sigma^+ \to p\gamma^*$ amplitude, they do not depend on t.

APPENDIX B: IMAGINARY PARTS OF FORM FACTORS IN χPT

The chiral Lagrangian for the interactions of the lowest-lying mesons and baryons is written down in terms of the lightest meson-octet and baryon-octet fields, which are collected into 3×3 matrices
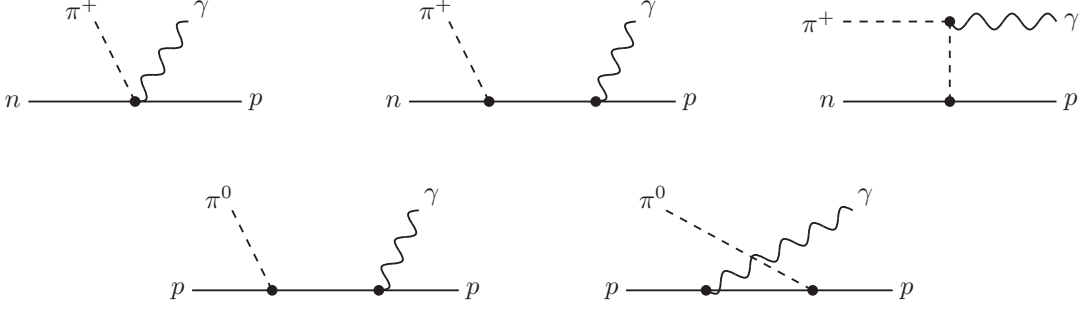
FIG. 6: Leading-order diagrams for $N\pi \to p\gamma^*$ reactions.

φ and B, respectively [13]. The mesons enter through the exponential $\Sigma = \xi^2 = \exp(i\varphi/f)$, where $f = f_\pi = 92.4\,\text{MeV}$ is the pion decay constant. In the relativistic baryon χPT, the lowest-order strong Lagrangian is given by [13]

$$\mathcal{L}_{\text{s}} = \langle \bar{B}\, i\gamma^\mu\big(\partial_\mu B + [\mathcal{V}_\mu, B]\big)\rangle + m_0 \langle \bar{B}B\rangle + D\langle \bar{B}\gamma^\mu\gamma_5 \{\mathcal{A}_\mu, B\}\rangle + F\langle \bar{B}\gamma^\mu\gamma_5 [\mathcal{A}_\mu, B]\rangle , \quad \text{(B1)}$$

where $\langle \cdots \rangle \equiv \text{Tr}(\cdots)$ in flavor space, m_0 is the baryon mass in the chiral limit, $\mathcal{V}^\mu = \frac{1}{2}\big(\xi\, \partial^\mu \xi^\dagger + \xi^\dagger\, \partial^\mu \xi\big) + \frac{i}{2}\, eA^\mu\big(\xi^\dagger Q\xi + \xi Q\xi^\dagger\big)$, and $\mathcal{A}^\mu = \frac{i}{2}\big(\xi\, \partial^\mu \xi^\dagger - \xi^\dagger\, \partial^\mu \xi\big) + \frac{1}{2}\, eA^\mu\big(\xi^\dagger Q\xi - \xi Q\xi^\dagger\big)$, with A^μ being the photon field and $Q = \text{diag}(2,-1,-1)/3$ the quark-charge matrix.[4] The parameters D and F will enter our results below only through the combination $D + F = 1.26$.

From $\mathcal{L}_{\text{s}}$ we derive two sets of diagrams, shown in Fig. 6, which represent the $N\pi \to p\gamma^*$ reactions involved in the unitarity calculation of the imaginary parts of the form factors a, b, c, and d. It then follows from Fig. 1 that the first set of diagrams is associated with the weak transition $\Sigma^+ \to n\pi^+$, and the second with $\Sigma^+ \to p\pi^0$. Consequently, we express our results as

$$\text{Im}\,\mathcal{F} = \frac{(D+F)m_{\pi^+}^2}{8\sqrt{2}\,\pi f_\pi}\left(\tilde{\mathcal{F}}_+ + \frac{\tilde{\mathcal{F}}_0}{\sqrt{2}}\right) \qquad \text{for}\ \ \mathcal{F} = a, b, c, d , \quad \text{(B2)}$$

where $\tilde{\mathcal{F}}_+$ $(\tilde{\mathcal{F}}_0)$ comes from the $n\pi^+$ $(p\pi^0)$ contribution, and write them in terms of the weak amplitudes $A_+ = A_{n\pi^+}$, $A_0 = A_{p\pi^0}$, $B_+ = B_{n\pi^+}$, and $B_0 = B_{p\pi^0}$ given in Eq. (18). Working in the Σ^+ rest-frame, which implies that the energies and momenta of the photon and proton in the final state and of the pion in the intermediate are fixed by kinematics, we define

$$z_+ = \left(\frac{2E_\pi E_\gamma - 2|\boldsymbol{p}_\pi|\,|\boldsymbol{p}_\gamma| - q^2}{2E_\pi E_\gamma + 2|\boldsymbol{p}_\pi|\,|\boldsymbol{p}_\gamma| - q^2}\right) , \qquad z_0 = \left(\frac{2E_\pi E_p - 2|\boldsymbol{p}_\pi|\,|\boldsymbol{p}_p| - m_\pi^2}{2E_\pi E_p + 2|\boldsymbol{p}_\pi|\,|\boldsymbol{p}_p| - m_\pi^2}\right) . \quad \text{(B3)}$$

---

[4] Under a chiral transformation, $\bar{B} \to U\bar{B}U^\dagger$, $B \to UBU^\dagger$, $\mathcal{V}^\mu \to U\mathcal{V}^\mu U^\dagger + i\partial^\mu U\, U^\dagger$, and $\mathcal{A}^\mu \to U\mathcal{A}^\mu U^\dagger$, where U is defined by $\xi \to L\xi U^\dagger = U\xi R^\dagger$.

The expression for $\tilde{\mathcal{F}}$ from each set of diagrams can then be written as

$$\tilde{a}_{+,0} = \frac{B_{+,0}\, m_N}{2m_\Sigma^2\, |\boldsymbol{p}_\gamma|} \frac{\left[2|\boldsymbol{p}_\pi|\,|\boldsymbol{p}_\gamma|\, f_{+,0}^{(a)} + \ln(z_{+,0})\, g_{+,0}^{(a)}\right]}{\left[(m_\Sigma - m_N)^2 - q^2\right]\left[(m_\Sigma + m_N)^2 - q^2\right]^2}\ ,$$

$$\tilde{b}_{+,0} = \frac{-A_{+,0}\, m_N}{2m_\Sigma^2\, |\boldsymbol{p}_\gamma|} \frac{\left[2|\boldsymbol{p}_\pi|\,|\boldsymbol{p}_\gamma|\, f_{+,0}^{(b)} + \ln(z_{+,0})\, g_{+,0}^{(b)}\right]}{\left[(m_\Sigma - m_N)^2 - q^2\right]^2\left[(m_\Sigma + m_N)^2 - q^2\right]}\ ,$$

$$\tilde{c}_{+,0} = \frac{B_{+,0}\, m_N}{2m_\Sigma^2\, |\boldsymbol{p}_\gamma|\,(m_N - m_\Sigma)} \frac{\left[2|\boldsymbol{p}_\pi|\,|\boldsymbol{p}_\gamma|\, f_{+,0}^{(c)} + \ln(z_{+,0})\, g_{+,0}^{(c)}\right]}{\left[(m_\Sigma - m_N)^2 - q^2\right]\left[(m_\Sigma + m_N)^2 - q^2\right]^2}\ ,$$

$$\tilde{d}_{+,0} = \frac{-A_{+,0}\, m_N}{2m_\Sigma^2\, |\boldsymbol{p}_\gamma|\,(m_\Sigma + m_N)} \frac{\left[2|\boldsymbol{p}_\pi|\,|\boldsymbol{p}_\gamma|\, f_{+,0}^{(d)} + \ln(z_{+,0})\, g_{+,0}^{(d)}\right]}{\left[(m_\Sigma - m_N)^2 - q^2\right]^2\left[(m_\Sigma + m_N)^2 - q^2\right]}\ , \tag{B4}$$

where

$$f_+^{(a)} = m_N m_\Sigma^5 + \left(q^2 + 2m_\pi^2 + m_N^2\right) m_\Sigma^4 - m_N\left(3q^2 - 3m_\pi^2 + 2m_N^2\right) m_\Sigma^3$$
$$- \left(q^4 - 5m_\pi^2 q^2 + 2m_N^4 + \left(q^2 + m_\pi^2\right) m_N^2\right) m_\Sigma^2$$
$$+ m_N\left(m_N^2 - q^2\right)\left(2q^2 - 3m_\pi^2 + m_N^2\right) m_\Sigma + \left(q^2 - m_N^2\right)^2\left(m_N^2 - m_\pi^2\right)\ ,$$

$$g_+^{(a)} = m_\Sigma\left(m_N q^6 + \left(m_N\left(2m_N - m_\Sigma\right)\left(m_N + m_\Sigma\right) - m_\pi^2\left(3m_N + m_\Sigma\right)\right) q^4\right.$$
$$\left. + m_\pi^2\left(3m_\pi^2 - 4m_N^2\right)\left(m_N + m_\Sigma\right) q^2 + m_\pi^2\left(m_N - m_\Sigma\right)^2\left(m_N + m_\Sigma\right)^3\right)\ ,$$

$$f_0^{(a)} = 3m_N m_\Sigma^5 - \left(q^2 - 2m_\pi^2 - 3m_N^2\right) m_\Sigma^4 - m_N\left(4m_N^2 - 3\left(q^2 + m_\pi^2\right)\right) m_\Sigma^3$$
$$+ \left(q^4 + 5m_\pi^2 q^2 - 4m_N^4 - \left(q^2 + m_\pi^2\right) m_N^2\right) m_\Sigma^2$$
$$+ m_N\left(m_N^2 - q^2\right)\left(2q^2 - 3m_\pi^2 + m_N^2\right) m_\Sigma + \left(q^2 - m_N^2\right)^2\left(m_N^2 - m_\pi^2\right)\ ,$$

$$g_0^{(a)} = m_\Sigma\left(-2m_\pi^2 m_\Sigma q^4 - \left(m_N + m_\Sigma\right)\left(3m_\pi^4 - 2\left(3m_N^2 - 2m_\Sigma m_N + m_\Sigma^2\right) m_\pi^2\right.\right.$$
$$\left.\left. + m_N\left(m_N - m_\Sigma\right)^2\left(3m_N + m_\Sigma\right)\right) q^2 + m_N\left(m_N - m_\Sigma\right)^2 m_\Sigma\left(m_N + m_\Sigma\right)^3\right)\ , \tag{B5a}$$

$$f_+^{(b)} = m_N m_\Sigma^5 - \left(q^2 + 2m_\pi^2 + m_N^2\right) m_\Sigma^4 - m_N\left(3q^2 - 3m_\pi^2 + 2m_N^2\right) m_\Sigma^3$$
$$+ \left(q^4 - 5m_\pi^2 q^2 + 2m_N^4 + \left(q^2 + m_\pi^2\right) m_N^2\right) m_\Sigma^2$$
$$+ m_N\left(m_N^2 - q^2\right)\left(2q^2 - 3m_\pi^2 + m_N^2\right) m_\Sigma + \left(q^2 - m_N^2\right)^2\left(m_\pi^2 - m_N^2\right)\ ,$$

$$g_+^{(b)} = -m_\Sigma\left(-m_N q^6 + \left(\left(3m_N - m_\Sigma\right) m_\pi^2 + m_N\left(-2m_N^2 + m_\Sigma m_N + m_\Sigma^2\right)\right) q^4\right.$$
$$\left. - m_\pi^2\left(3m_\pi^2 - 4m_N^2\right)\left(m_N - m_\Sigma\right) q^2 - m_\pi^2\left(m_N - m_\Sigma\right)^3\left(m_N + m_\Sigma\right)^2\right)\ ,$$

$$f_0^{(b)} = 3m_N m_\Sigma^5 + \left(q^2 - 2m_\pi^2 - 3m_N^2\right) m_\Sigma^4 + m_N\left(3\left(q^2 + m_\pi^2\right) - 4m_N^2\right) m_\Sigma^3$$
$$- \left(q^4 + 5m_\pi^2 q^2 - 4m_N^4 - \left(q^2 + m_\pi^2\right) m_N^2\right) m_\Sigma^2$$
$$+ m_N\left(m_N^2 - q^2\right)\left(2q^2 - 3m_\pi^2 + m_N^2\right) m_\Sigma + \left(q^2 - m_N^2\right)^2\left(m_\pi^2 - m_N^2\right)\ ,$$

$$g_0^{(b)} = -m_\Sigma\left(-2m_\pi^2 m_\Sigma q^4 + \left(m_N - m_\Sigma\right)\left(3m_\pi^4 - 2\left(3m_N^2 + 2m_\Sigma m_N + m_\Sigma^2\right) m_\pi^2\right.\right.$$
$$\left.\left. + m_N\left(3m_N - m_\Sigma\right)\left(m_N + m_\Sigma\right)^2\right) q^2 + m_N\left(m_N - m_\Sigma\right)^3 m_\Sigma\left(m_N + m_\Sigma\right)^2\right)\ , \tag{B5b}$$

14

$$f_+^{(c)} = m_\pi^2 \left(8m_\Sigma^4 + 5m_N m_\Sigma^3 - \left(3q^2 + m_N^2\right) m_\Sigma^2 + 3m_N \left(m_N^2 - q^2\right) m_\Sigma + \left(q^2 - m_N^2\right)^2\right)$$
$$- \left(m_N - m_\Sigma\right)\left(-m_N m_\Sigma^4 + \left(q^2 - 2m_N^2\right) m_\Sigma^3 - 4q^2 m_N m_\Sigma^2\right.$$
$$\left. - \left(q^4 + m_N^2 q^2 - 2m_N^4\right) m_\Sigma + m_N \left(q^2 - m_N^2\right)^2\right) ,$$

$$g_+^{(c)} = -\left(m_N - m_\Sigma\right) m_\Sigma \left(m_N \left(2m_N + m_\Sigma\right) q^4 + \left(m_\pi^4 - 2\left(3m_N^2 + 2m_\Sigma m_N + m_\Sigma^2\right) m_\pi^2\right.\right.$$
$$\left.\left. + m_N \left(m_N - m_\Sigma\right)\left(m_N + m_\Sigma\right)^2\right) q^2 + 2m_\pi^2 \left(m_N + m_\Sigma\right)^2 \left(m_\pi^2 + m_\Sigma \left(m_\Sigma - m_N\right)\right)\right) ,$$

$$f_0^{(c)} = m_\pi^2 \left(8m_\Sigma^4 + 5m_N m_\Sigma^3 - \left(3q^2 + m_N^2\right) m_\Sigma^2 + 3m_N \left(m_N^2 - q^2\right) m_\Sigma + \left(q^2 - m_N^2\right)^2\right)$$
$$- \left(m_N - m_\Sigma\right)^2 \left(2m_\Sigma^4 - m_N m_\Sigma^3 - \left(3q^2 + m_N^2\right) m_\Sigma^2 + 3m_N \left(m_N^2 - q^2\right) m_\Sigma\right.$$
$$\left. + \left(q^2 - m_N^2\right)^2\right) ,$$

$$g_0^{(c)} = \left(m_N - m_\Sigma\right) m_\Sigma \left(\left(m_\pi^4 - \left(2m_N^2 - 4m_\Sigma m_N - 2m_\Sigma^2\right) m_\pi^2 + m_N \left(m_N - m_\Sigma\right)^2 \left(m_N + m_\Sigma\right)\right) q^2\right.$$
$$\left. + \left(m_N + m_\Sigma\right)^2 \left(2m_\pi^4 - 2\left(2m_N^2 - m_\Sigma m_N + m_\Sigma^2\right) m_\pi^2 + m_N \left(m_N - m_\Sigma\right)^2 \left(2m_N - m_\Sigma\right)\right)\right) , \tag{B5c}$$

$$f_+^{(d)} = \left(m_N + m_\Sigma\right)\left(-m_N m_\Sigma^4 - \left(q^2 - 2m_N^2\right) m_\Sigma^3 - 4q^2 m_N m_\Sigma^2\right.$$
$$\left. + \left(q^4 + m_N^2 q^2 - 2m_N^4\right) m_\Sigma + m_N \left(q^2 - m_N^2\right)^2\right)$$
$$- m_\pi^2 \left(8m_\Sigma^4 - 5m_N m_\Sigma^3 - \left(3q^2 + m_N^2\right) m_\Sigma^2 + 3m_N \left(q^2 - m_N^2\right) m_\Sigma + \left(q^2 - m_N^2\right)^2\right) ,$$

$$g_+^{(d)} = m_\Sigma \left(m_N + m_\Sigma\right) \left(-m_N \left(2m_N - m_\Sigma\right) q^4 - \left(m_\pi^4 - 2\left(3m_N^2 - 2m_\Sigma m_N + m_\Sigma^2\right) m_\pi^2\right.\right.$$
$$\left.\left. + m_N \left(m_N - m_\Sigma\right)^2 \left(m_N + m_\Sigma\right)\right) q^2 - 2m_\pi^2 \left(m_N - m_\Sigma\right)^2 \left(m_\pi^2 + m_\Sigma \left(m_N + m_\Sigma\right)\right)\right) ,$$

$$f_0^{(d)} = \left(m_N + m_\Sigma\right)^2 \left(2m_\Sigma^4 + m_N m_\Sigma^3 - \left(3q^2 + m_N^2\right) m_\Sigma^2 + 3m_N \left(q^2 - m_N^2\right) m_\Sigma + \left(q^2 - m_N^2\right)^2\right)$$
$$- m_\pi^2 \left(8m_\Sigma^4 - 5m_N m_\Sigma^3 - \left(3q^2 + m_N^2\right) m_\Sigma^2 + 3m_N \left(q^2 - m_N^2\right) m_\Sigma + \left(q^2 - m_N^2\right)^2\right) ,$$

$$g_0^{(d)} = m_\Sigma \left(m_N + m_\Sigma\right) \left(\left(m_\pi^4 - 2\left(m_N^2 + 2m_\Sigma m_N - m_\Sigma^2\right) m_\pi^2 + m_N \left(m_N - m_\Sigma\right)\left(m_N + m_\Sigma\right)^2\right) q^2\right.$$
$$+ \left(m_N - m_\Sigma\right)^2 \left(2m_\pi^4 - 2\left(2m_N^2 + m_\Sigma m_N + m_\Sigma^2\right) m_\pi^2\right.$$
$$\left.\left. + m_N \left(m_N + m_\Sigma\right)^2 \left(2m_N + m_\Sigma\right)\right)\right) . \tag{B5d}$$

In our numerical computations, $m_\Sigma = m_{\Sigma^+}$, $m_N = \frac{1}{2}\left(m_p + m_n\right)$, $m_\pi = \frac{1}{3}\left(2m_{\pi^+} + m_{\pi^0}\right)$, the numbers being from Ref. [8].

In heavy baryon χPT [14], the relevant Lagrangian can be found in Ref. [10], and the weak radiative and nonleptonic amplitudes in Eqs. (10) and (17) become, respectively,

$$\mathcal{M}(B_i \to B_f \gamma^*) = -eG_F \, \bar{B}_f \left[2\left(S \cdot q \, S^\mu - S^\mu S \cdot q\right) a + 2\left(S \cdot q \, v^\mu - S^\mu v \cdot q\right) b\right] B_i \, \varepsilon_\mu^*$$
$$- eG_F \, \bar{B}_f \left[\left(q^2 \, v^\mu - q^\mu \, v \cdot q\right) c + 2\left(q^2 \, S^\mu - q^\mu S \cdot q\right) d\right] B_i \, \varepsilon_\mu^* , \tag{B6}$$

$$\mathcal{M}(\Sigma^+ \to N\pi) = iG_F m_{\pi^+}^2 \, \bar{N} \left(A_{N\pi} + 2S \cdot p_\pi \frac{B_{N\pi}}{2m_\Sigma}\right) \Sigma , \tag{B7}$$

where v is the baryon four-velocity and S is the baryon spin operator. Following Ref. [10], to obtain the imaginary parts of the form factors we evaluate the loop diagrams displayed in Fig. 7. In the heavy-baryon approach, only the diagrams with the $\Sigma^+ \to n\pi^+$ transition yield nonzero contributions to the leading-order imaginary parts. The results are

$$
\begin{aligned}
\operatorname{Im} a = \frac{(D+F)\, m_{\pi^+}^2}{8\sqrt{2}\,\pi f_\pi} \frac{B_{n\pi^+}}{2m_\Sigma} & \left\{ \sqrt{\Delta^2 - m_\pi^2}\left(1 + \frac{\frac{1}{2}q^2}{\Delta^2 - q^2}\right) \right. \\
& \left. + \frac{q^4 + 4m_\pi^2(\Delta^2 - q^2)}{4(\Delta^2 - q^2)^{3/2}} \ln\left[\frac{2\Delta^2 - q^2 - 2\sqrt{\Delta^2 - m_\pi^2}\sqrt{\Delta^2 - q^2}}{\sqrt{q^4 + 4m_\pi^2(\Delta^2 - q^2)}}\right] \right\} ,
\end{aligned}
\tag{B8a}
$$

$$
\begin{aligned}
\operatorname{Im} b = \frac{(D+F)\, m_{\pi^+}^2}{8\sqrt{2}\,\pi f_\pi} A_{n\pi^+} & \left\{ \frac{-\Delta\sqrt{\Delta^2 - m_\pi^2}}{\Delta^2 - q^2}\left(1 - \frac{\frac{3}{2}q^2}{\Delta^2 - q^2}\right) \right. \\
& \left. + \Delta\frac{3q^4 + 4m_\pi^2(\Delta^2 - q^2)}{4(\Delta^2 - q^2)^{5/2}} \ln\left[\frac{2\Delta^2 - q^2 - 2\sqrt{\Delta^2 - m_\pi^2}\sqrt{\Delta^2 - q^2}}{\sqrt{q^4 + 4m_\pi^2(\Delta^2 - q^2)}}\right] \right\} ,
\end{aligned}
\tag{B8b}
$$

$$
\begin{aligned}
\operatorname{Im} c = \frac{(D+F)\, m_{\pi^+}^2}{8\sqrt{2}\,\pi f_\pi} \frac{B_{n\pi^+}}{2m_\Sigma} & \left\{ \sqrt{\Delta^2 - m_\pi^2}\frac{\Delta^2 - 2m_\pi^2}{\Delta(\Delta^2 - q^2)} \right. \\
& \left. + \frac{\Delta(q^2 - 2m_\pi^2)}{2(\Delta^2 - q^2)^{3/2}} \ln\left[\frac{2\Delta^2 - q^2 - 2\sqrt{\Delta^2 - m_\pi^2}\sqrt{\Delta^2 - q^2}}{\sqrt{q^4 + 4m_\pi^2(\Delta^2 - q^2)}}\right] \right\} ,
\end{aligned}
\tag{B8c}
$$

$$
\begin{aligned}
\operatorname{Im} d = \frac{(D+F)\, m_{\pi^+}^2}{8\sqrt{2}\,\pi f_\pi} A_{n\pi^+} & \left\{ \sqrt{\Delta^2 - m_\pi^2}\frac{\frac{3}{2}q^2}{(\Delta^2 - q^2)^2} \right. \\
& \left. + \frac{q^4 + 2q^2\Delta^2 + 4m_\pi^2(\Delta^2 - q^2)}{4(\Delta^2 - q^2)^{5/2}} \ln\left[\frac{2\Delta^2 - q^2 - 2\sqrt{\Delta^2 - m_\pi^2}\sqrt{\Delta^2 - q^2}}{\sqrt{q^4 + 4m_\pi^2(\Delta^2 - q^2)}}\right] \right\} ,
\end{aligned}
\tag{B8d}
$$

where $\Delta = m_\Sigma - m_N$. We have checked that these formulas can be reproduced from the relativistic results in Eq. (B2) by expanding the latter in terms of Δ/m_Σ, $\sqrt{q^2}/m_\Sigma$, and m_π/m_Σ and keeping the leading nonzero terms.
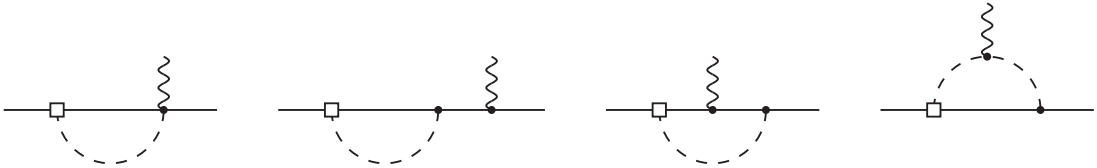

FIG. 7: Diagrams for imaginary part of $\Sigma^+ \to p\gamma^*$ amplitude.

APPENDIX C: REAL PARTS OF $c(q^2)$ AND $d(q^2)$

Vector mesons can contribute to c via the pole diagrams shown in Fig. 8(a). The strong vertices in the diagrams come from the Lagrangian [15, 16]

$$\mathcal{L}'_s = \mathcal{G}_D \left\langle \bar{B} \gamma^\mu \left\{ \mathsf{V}_\mu, B \right\} \right\rangle + \mathcal{G}_F \left\langle \bar{B} \gamma^\mu \left[\mathsf{V}_\mu, B \right] \right\rangle + \mathcal{G}_0 \left\langle \bar{B} \gamma^\mu B \right\rangle \left\langle \mathsf{V}_\mu \right\rangle$$
$$- \tfrac{1}{2} e f_\mathsf{V} \left\langle \left(D^\mu \mathsf{V}^\nu - D^\nu \mathsf{V}^\mu \right) \left(\xi^\dagger Q \xi + \xi Q \xi^\dagger \right) \right\rangle \left(\partial_\mu A_\nu - \partial_\nu A_\mu \right) , \qquad \text{(C1)}$$

with $\mathsf{V} = \tfrac{1}{2}\lambda_3 \rho^0 + \cdots$ containing the nonet of vector-meson fields and $D^\mu \mathsf{V}^\nu = \partial^\mu \mathsf{V}^\nu + \left[\mathcal{V}^\mu, \mathsf{V}^\nu \right]$,[5] whereas the weak vertices arise from

$$\mathcal{L}_\mathrm{w} = G_\mathrm{F} m_{\pi^+}^2 \left(h_D \left\langle \bar{B} \left\{ \xi^\dagger h \xi, B \right\} \right\rangle + h_F \left\langle \bar{B} \left[\xi^\dagger h \xi, B \right] \right\rangle + h_\mathsf{V} \left\langle h \, \xi \mathsf{V}^\mu \mathsf{V}_\mu \xi^\dagger \right\rangle \right) + \text{H.c.} , \qquad \text{(C2)}$$

with h being a 3×3-matrix having elements $h_{kl} = \delta_{k2} \delta_{3l}$ which selects out $s \to d$ transitions. The relevant parameters in $\mathcal{L}'_s$ are $\mathcal{G}_D = -13.9$ and $\mathcal{G}_F = 17.9$ from a recent dispersive analysis [16, 17],[6] and $f_\mathsf{V} = 0.201$ from $\rho^0 \to e^+ e^-$ rate [8], while those in $\mathcal{L}_\mathrm{w}$ are $h_D = -72 \,\mathrm{MeV}$ and $h_F = 179 \,\mathrm{MeV}$ extracted at tree level from S-wave hyperon nonleptonic decays [18], but h_V cannot be determined directly from data. To estimate h_V, we use the $\mathrm{SU(6)}_w$ relation $\left\langle \pi^0 \middle| \mathcal{H}_\mathrm{w} \middle| \bar{K}^0 \right\rangle = \left\langle \rho^0 \middle| \mathcal{H}_\mathrm{w} \middle| \bar{K}^{*0} \right\rangle$ derived in Ref. [19]. Thus, employing the weak chiral Lagrangian $\mathcal{L}^\varphi_\mathrm{w} = \gamma_8 f^2 \left\langle h \, \partial^\mu \Sigma \, \partial_\mu \Sigma^\dagger \right\rangle + \text{H.c.}$,
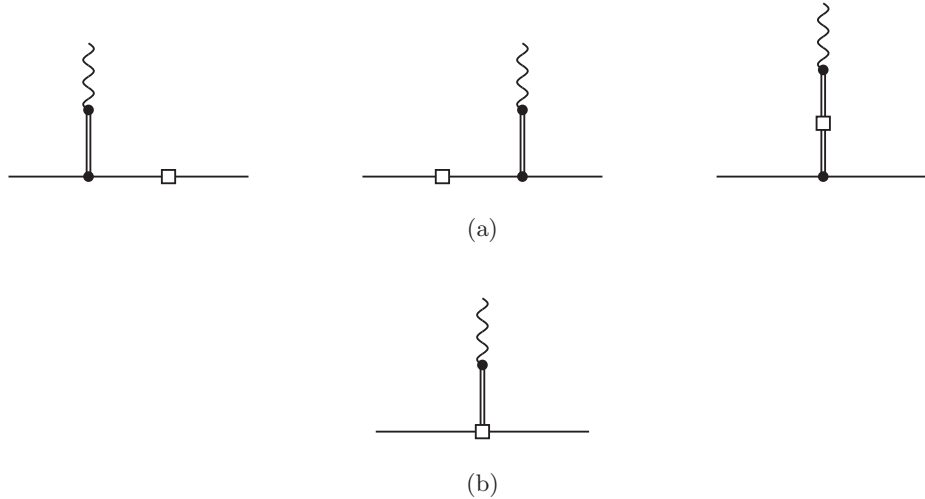

(a)

(b)

FIG. 8: Pole diagrams contributing to the c and d amplitudes. A single line (double line) denotes a baryon (vector meson) field, and a solid dot (hollow square) represents a strong (weak) vertex.

---

[5] Under a chiral transformation, $\mathsf{V} \to U \mathsf{V} U^\dagger$ and $D^\mu \mathsf{V}^\nu \to U D^\mu \mathsf{V}^\nu U^\dagger$.

[6] Although $\mathcal{G}_0$ does not appear in our results, it enters the extraction of $\mathcal{G}_{D,F}$. Writing the ppV part of $\mathcal{L}'_s$ as $\tfrac{1}{2} \bar{p} \gamma^\mu p \left(g_{\rho NN} \rho^0_\mu + g_{\omega NN} \omega_\mu + g_{\phi NN} \phi_\mu \right)$, we have $g_{\rho NN} = \mathcal{G}_D + \mathcal{G}_F = 4.0$, $g_{\omega NN} = \mathcal{G}_D + \mathcal{G}_F + 2\mathcal{G}_0 = 41.8$, and $g_{\phi NN} = \sqrt{2} \left(\mathcal{G}_D - \mathcal{G}_F + \mathcal{G}_0 \right) = -18.3$, where the numbers are from Ref. [16, 17].

with $\gamma_8 = 7.8 \times 10^{-8}$ from $K \to \pi\pi$ data, we find $h_V = -4\gamma_8 \, m_K^2/(G_F m_{\pi^+}^2) = -0.34 \, \mathrm{GeV}^2$. Putting things together and adopting ideal ω-ϕ mixing, we then obtain

$$\mathrm{Re}\, c = \frac{f_V \left(\mathcal{G}_D - \mathcal{G}_F\right) m_{\pi^+}^2 \left(h_D - h_F\right)}{6\left(m_\Sigma - m_N\right)} \left(\frac{3}{q^2 - m_\rho^2} - \frac{1}{q^2 - m_\omega^2} - \frac{2}{q^2 - m_\phi^2}\right)$$

$$+ \frac{f_V \left(\mathcal{G}_D - \mathcal{G}_F\right) m_{\pi^+}^2 \, h_V}{12\left(q^2 - m_{K^*}^2\right)} \left(\frac{3}{q^2 - m_\rho^2} - \frac{1}{q^2 - m_\omega^2} + \frac{2}{q^2 - m_\phi^2}\right) \ . \tag{C3}$$

The form factor d can receive vector-meson contributions from the parity-violating Lagrangian

$$\mathcal{L}'_w = G_F m_{\pi^+}^2 \, h_{PV} \left\langle h\,\xi \left\{\left[\bar{B}, \gamma^\mu \gamma_5 B\right], \mathsf{V}_\mu\right\} \xi^\dagger \right\rangle + \text{H.c.} \ , \tag{C4}$$

which are represented by the diagram in Fig. 8(b). The parameter h_{PV} also cannot be fixed directly from data, and so we estimate it by adopting again the $\mathrm{SU}(6)_w$ results of Ref. [19] to be $h_{PV} = 2.41$. It follows that

$$\mathrm{Re}\, d = \frac{f_V \, m_{\pi^+}^2 \, h_{PV}}{6} \left(\frac{3}{q^2 - m_\rho^2} - \frac{1}{q^2 - m_\omega^2} + \frac{2}{q^2 - m_\phi^2}\right) \ . \tag{C5}$$

---

[1] H. Park *et al.* [HyperCP Collaboration], Phys. Rev. Lett. **94**, 021801 (2005) [arXiv:hep-ex/0501014].

[2] L. Bergstrom, R. Safadi, and P. Singer, Z. Phys. C **37**, 281 (1988).

[3] G. Buchalla, A.J. Buras, and M.E. Lautenbacher, Rev. Mod. Phys. **68**, 1125 (1996) [arXiv:hep-ph/9512380].

[4] X.G. He and G. Valencia, Phys. Rev. D **61**, 075003 (2000) [arXiv:hep-ph/9908298].

[5] M.A. Shifman, A.I. Vainshtein, and V.I. Zakharov, Phys. Rev. D **18**, 2583 (1978) [Erratum-ibid. D **19**, 2815 (1979)].

[6] N. Cabibbo, Phys. Rev. Lett. **10**, 531 (1963); M. Kobayashi and T. Maskawa, Prog. Theor. Phys. **49**, 652 (1973).

[7] J.F. Donoghue, E. Golowich, and B.R. Holstein, *Dynamics of the Standard Model* (Cambridge University Press, Cambridge, 1992).

[8] S. Eidelman *et al.* [Particle Data Group], Phys. Lett. B **592**, 1 (2004).

[9] H. Neufeld, Nucl. Phys. B **402**, 166 (1993).

[10] E. Jenkins, M.E. Luke, A.V. Manohar, and M.J. Savage, Nucl. Phys. B **397**, 84 (1993) [arXiv:hep-ph/9210265].

[11] J.W. Bos *et al.*, Phys. Rev. D **54**, 3321 (1996) [arXiv:hep-ph/9601299]; *ibid.* **57**, 4101 (1998) [arXiv:hep-ph/9611260].

[12] G. Ang *et al.*, Z. Phys. **228**, 151 (1969).

[13] J. Bijnens, H. Sonoda, and M.B. Wise, Nucl. Phys. B **261**, 185 (1985).

[14] E. Jenkins and A.V. Manohar, Phys. Lett. B **255**, 558 (1991); in *Effective Field Theories of the Standard Model*, edited by U.-G. Meissner (World Scientific, Singapore, 1992).

[15] G. Ecker *et al.*, Phys. Lett. B **223**, 425 (1989); B. Borasoy and U.G. Meissner, Int. J. Mod. Phys. A **11**, 5183 (1996) [arXiv:hep-ph/9511320].

[16] B. Kubis and U.G. Meissner, Nucl. Phys. A **679**, 698 (2001) [arXiv:hep-ph/0007056].

[17] P. Mergell, U.G. Meissner, and D. Drechsel, Nucl. Phys. A **596**, 367 (1996) [arXiv:hep-ph/9506375];

[18] A. Abd El-Hady and J. Tandean, Phys. Rev. D **61**, 114014 (2000) [arXiv:hep-ph/9908498].

[19] J.F. Dubach, G.B. Feldman, and B.R. Holstein, Annals Phys. **249**, 146 (1996) [arXiv:nucl-th/9606003].